

Doped two orbital chains with strong Hund's rule couplings - ferromagnetism, spin gap, singlet and triplet pairings

Beat AMMON * and Masatoshi IMADA **

ISSP, University of Tokyo, 7-22-1 Roppongi, Minato-ku, Tokyo 106-8666, Japan

(Received November 3, 2018)

Different models for doping of two-orbital chains with mobile $S = 1/2$ fermions and strong, ferromagnetic (FM) Hund's rule couplings stabilizing the $S = 1$ spins are investigated by density matrix renormalization group (DMRG) methods. The competition between antiferromagnetic (AF) and FM order leads to a rich phase diagram with a narrow FM region for weak AF couplings and strongly enhanced triplet pairing correlations. Without a level difference between the orbitals, the spin gap persists upon doping, whereas gapless spin excitations are generated by interactions among itinerant polarons in the presence of a level difference. In the charge sector we find dominant singlet pairing correlations without a level difference, whereas upon the inclusion of a Coulomb repulsion between the orbitals or with a level difference, charge density wave (CDW) correlations decay slowest. The string correlation functions remain finite upon doping for all models.

KEYWORDS: spin-1 systems, Mott-Hubbard transition, superconductivity, triplet superconductivity, ferromagnetism, string order

§1. Introduction

A key problem in the research on the Mott-Hubbard transition consists of the doping of a spin liquid ground-state with mobile holes. The antiferromagnetic (AF) $S = 1$ Heisenberg (HB) spin chain is an example of such a spin liquid with a finite spin gap¹⁾ and a hidden topological order, the string correlation function.²⁾ Doping of $S = 1$ HB chains poses a number of interesting theoretical questions caused by the competition between ferromagnetic (FM) order induced by the double exchange mechanism³⁾ and AF order which can result in completely different magnetic properties. Another relevant question is whether the spin gap is destroyed immediately upon doping or whether it persists, and the competition also determines which correlation function characterized by the single correlation exponent K_ρ dominates in the thermodynamic limit of infinite system size.

Only recently has it become possible to experimentally study mobile holes doped in a $S = 1$ chain in the system $Y_{2-x}Ca_xBaNiO_5$.⁴⁾ The two active Ni^+ orbitals are the $3d_{3z^2-r^2}$ and the almost localized $3d_{x^2-y^2}$ orbital. Strong Hund's rule couplings J_H between these two orbitals and very weak inter-chain couplings make this system an almost ideal $S = 1$ HB chain with a spin gap of $\Delta_s \approx 100K$ in the undoped case.⁵⁾ By replacing off-chain Y^{3+} with Ca^{2+} , mobile holes can be introduced into the system and μ SR data show that these carriers indeed have spin $S = 1/2$.⁶⁾ The most interesting experimental features upon doping consist of a reduction of the resistivity ρ_{dc} by several orders of magnitude and that the temperature dependence of ρ_{dc} no longer can be

described by thermal activation over a barrier.⁴⁾ Further new states with spin S between 1 and $3/2$ per impurity appear below the Haldane gap.⁴⁾

First theoretical studies on doped $S = 1$ chains concentrated on localized $S = 1/2$ impurities.⁷⁾ For sufficiently weak couplings, they give rise to bound $S = 1/2$ states below the Haldane-gap,⁸⁾ similar to the chain-end excitations.⁹⁾ However, it soon turned out that mobile carriers are needed for an accurate description of this system and the case of weak hopping¹⁰⁾ has been studied first. A more realistic effective Hamiltonian for fully mobile holes has been derived in¹¹⁾ for one- and two-band models with infinitely strong Hund's rule couplings. A phase diagram which shows a FM region and phase separation for large values of the coupling J between the $S = 1$ spins has been obtained by exact diagonalization and (DMRG) studies of small systems.¹²⁾ This study also suggests a possible hole-bound region between the FM and phase separated ones. Based on DMRG calculations for very large systems, we briefly have reported in a previous Letter on a new hierarchy of energy scales for a model with finite Hund's rule couplings including fully mobile holes and localized electrons in the lower band.¹³⁾ Ferromagnetic polarons formed by the double exchange mechanism are found to weakly interact in the lower energy scale in the background of the gapped spin liquid formed at the higher energy. Moreover, doping-induced magnetization steps have been discovered for an exactly solvable model which includes biquadratic exchange.¹⁴⁾ The biquadratic terms are needed for the solution by the algebraic Bethe Ansatz.

While all of the above mentioned studies are restricted to models with mobile electrons in the upper band only, the very different behavior of systems with and without a level difference between the two orbitals has first

* E-mail address: ammon@issp.u-tokyo.ac.jp

** E-mail address: imada@issp.u-tokyo.ac.jp

been investigated by weak-coupling theories.^{15,16} These studies show that the spin gap remains finite if there is no level difference between the orbitals, whereas the spin gap is destroyed immediately if the particle density between the two orbitals differs. We have recently carried out the first study of this problem in the strong coupling regime by numerical methods and discovered dominant superconducting pairing correlations for systems without a level difference in contrast to dominant charge-density wave (CDW) correlations for systems with a level difference.¹⁷ This surprising result which exhibits completely different phases depending on the level difference emphasizes the importance of a detailed study of realistic models in the strong coupling regime. Unfortunately this is also the most difficult regime to investigate, and it is not clear whether additional terms need to be included in a realistic model.

In this paper we present a detailed analysis of a realistic model in the strong coupling regime with strong but finite Hund's rule couplings J_F and fully mobile holes. Based on large scale numerical calculations by both the thermal DMRG (TDMRG)¹⁸ and ground state DMRG method,^{19,20} we will cover what has been left out due to lack of space in our two previous publications. In addition, we include a model with a Coulomb repulsion and no level difference between the electrons in the two orbitals on the same site.

We start with the discussion of a generic model for $Y_{2-x}Ca_xBaNiO_5$ which includes a level difference between the two orbitals, and we will call this the asymmetric model in the following. In this case, the electrons in the lower $3d_{x^2-y^2}$ orbital are almost localized, and all holes are doped into the higher lying $3d_{3z^2-r^2}$ orbital. We describe these mobile holes in the upper band by the following Hamiltonian:

$$H_{\text{kin}}^{(i)} = -t \sum_{j,\sigma} \mathcal{P} \left(c_{j,i,\sigma}^\dagger c_{j+1,i,\sigma} + H.c. \right) \mathcal{P}, \quad (1.1)$$

where the projection operator \mathcal{P} prohibits doubly occupied sites, $c_{j,i,\sigma}^\dagger$ is the particle creation operator on site j in the orbital i with spin σ , and the index $i = 1$ denotes the upper orbital and $i = 2$ the lower orbital. Due to virtual hopping processes there exist AF couplings $J > 0$ between nearest-neighbors in the upper band, and we include further AF couplings $J_d > 0$ between the electrons in different orbitals on neighboring sites as follows:

$$H_{\text{af}}^{(i)} = J \sum_j \left(\vec{S}_{j,i} \vec{S}_{j+1,i} - \frac{1}{4} n_{j,i} n_{j+1,i} \right) \quad (1.2)$$

$$H_{\text{diag}} = J_d \sum_j \left(\vec{S}_{j,1} \vec{S}_{j+1,2} + \vec{S}_{j,2} \vec{S}_{j+1,1} - \frac{1}{2} n_{j,1} n_{j+1,2} \right), \quad (1.3)$$

where the indices are the same as before, $n_{j,i} = c_{j,i,\uparrow}^\dagger c_{j,i,\uparrow} + c_{j,i,\downarrow}^\dagger c_{j,i,\downarrow}$, and the rest of the notation is standard. The strong Hund's rule coupling $J_H < 0$ between the electrons in different orbitals on the same site reads:

$$H_{\text{FM}} = J_H \sum_j \vec{S}_{j,1} \vec{S}_{j,2}, \quad (1.4)$$

and is responsible for the formation of the $S = 1$ spins. Finally the Hamiltonian for a model with a level difference is expressed as:

$$H_{\text{as}} = H_{\text{FM}} + H_{\text{diag}} + H_{\text{af}}^{(1)} + H_{\text{kin}}^{(1)}. \quad (1.5)$$

This model is easy to understand in two limiting cases: first at half filling, where it can be mapped to a Haldane $S = 1$ chain with a spin liquid ground state and a finite spin gap. The second case is away from half-filling at $J = J_d = 0$, where all the spins are ferromagnetically aligned due to the double-exchange mechanism in order to gain kinetic energy. Hence, for finite values of J, J_d there is a competition between FM order induced by the double exchange mechanism and the spin liquid ground state. For $|J_H| \gg J, J_d$ each hole is surrounded by a small FM cloud created by the double exchange mechanism, and we will call this a polaron in the following. An intriguing question on the doped system for small J and J_d is the possibility of triplet pairing. In this paper we show a strong enhancement of the triplet pairing correlations. However, for $J, J_d > 0.1t$, ferromagnetic polaron becomes only a weak perturbation of the underlying spin liquid which remains intact. Among these polarons $2k_F$ and $4k_F$ charge density wave (CDW) order is then stabilized. A hierarchy of energy scales is established in the spin sector with the smaller scale given by the gapless, lowest-lying interactions among the polarons; and the second, larger energy-scale consists of the spin liquid background.

On the other hand, we can think of a model with a very small or no level difference at all. This situation is more likely in a ladder-system, and we will refer to this model as the symmetric model in the following. From the symmetric model we include hopping and AF couplings $J > 0$ in both orbitals, and the Hamiltonian is given by:

$$H_{\text{sym}} = H_{\text{FM}} + H_{\text{diag}} + \sum_i \left(H_{\text{af}}^{(i)} + H_{\text{kin}}^{(i)} \right). \quad (1.6)$$

In this model the double exchange mechanism is expected to be less effective, since hole pairs on the same rung can gain the large Hund's rule coupling J_H . However, in many realistic situations there might be an additional Coulomb repulsion between the electrons on the same rung, and we will include this by the following additional term:

$$H_{\text{rep}} = U \sum_j n_{j,1} n_{j,2}. \quad (1.7)$$

This Coulomb repulsion will reestablish the competition between the double-exchange mechanism and the spin liquid ground state, while preserving the same particle density in both orbitals.

For all the models we restrict our investigations to the case of strong Hund's rule couplings $|J_H| \gg |J|, |J_d|, |t|$, and if not otherwise mentioned we always set $-J_H = 10t = 20J = 20J_d$, and $U = |J_H|$ for the model with a Coulomb repulsion between the electrons on the same site.

The rest of this paper is organized as follows: we start with a discussion of the numerical methods first. In the

next section we investigate various physical quantities in detail, and we begin with the discussion of the spin gap. There we see that the spin gap is destroyed immediately upon doping for the asymmetric model, while it remains finite for the symmetric models. Consistent with these findings we obtain finite values of the magnetic susceptibility χ for $T \rightarrow 0$ for the asymmetric model. We continue with the study of several correlation functions obtained by the DMRG method, and from the correlation exponent K_ρ obtained by fitting to the asymptotic form of a Tomonaga-Luttinger liquid in the gapless and a Luther-Emery liquid in the gapful case, we find that superconducting pairing correlations dominate in the thermodynamic limit of infinite system size for the symmetric model without Coulomb repulsion, while CDW correlations dominate in the two other cases. Finally, we investigate ferromagnetism and triplet pairing correlations for small values of the AF couplings J, J_d , and the last section of this report is devoted to the conclusion.

§2. Numerical Methods

In order to take the strong correlation effects into account properly, unbiased and approximation free methods are required, and large system-sizes are needed to avoid finite-size effects. For the investigation of the thermodynamic properties, we use the novel TDMRG method.¹⁸⁾ This method is based on the combination of the transfer matrix method²¹⁾ and the DMRG method. The TDMRG method allows us to reach temperatures as low as $T = 0.02t$ in the thermodynamic limit of infinite system size; and the only two sources of errors stem from the truncation errors of the DMRG procedure and the finite size of the Trotter time steps.

In order to apply the transfer matrix method we first map a one-dimensional quantum system to a two-dimensional classical system by the Trotter-Suzuki decomposition.²²⁾ For this purpose we decompose the Hamiltonian into two parts $H = H_{\text{odd}} + H_{\text{even}}$ where each $H_{\text{odd}(\text{even})}$ is a sum of commuting terms $H_{\text{odd}} = \sum_{i=1}^{L/2} h_{2i-1,2i}$ and $H_{\text{even}} = \sum_{i=1}^{L/2} h_{2i,2i+1}$. We then write the partition function of a system with L sites as

$$Z_L = \text{tr} e^{-\beta H} = \lim_{N \rightarrow \infty} Z_{N,L} \quad (2.1)$$

with $Z_{N,L} = \text{tr} (e^{-\beta H_{\text{odd}}/N} e^{-\beta H_{\text{even}}/N})^N$ and $\beta = 1/T$. With the definition of the virtual transfer-matrix $\mathcal{T}_i = (e^{-\beta h_{2i-1,2i}/N} e^{-\beta h_{2i,2i+1}/N})^N$ we obtain $Z_{N,L} = \lim_{N \rightarrow \infty} \text{tr} \prod_{i=1,L} \mathcal{T}_i$. By applying the Trotter-Suzuki interchangeability theorem²²⁾ we can exchange the limit of the system size with the limit of the Trotter number and obtain the free energy density f in the thermodynamic limit of infinite system size

$$\begin{aligned} f &= \lim_{N \rightarrow \infty} \lim_{L \rightarrow \infty} \left(-\frac{1}{\beta L} \right) \ln \text{tr} \prod_{i=1,L} \mathcal{T}_i \\ &= \lim_{N \rightarrow \infty} \left(-\frac{1}{\beta} \right) \ln \lambda_{\text{max}}, \end{aligned} \quad (2.2)$$

where λ_{max} is the maximum eigenvalue of \mathcal{T}_i . We can then calculate the maximum eigenvalue λ_{max} numerically and obtain physical quantities from derivatives of f . In

the actual calculations, several thermodynamic quantities such as the internal energy u or the magnetization m are obtained directly from the maximal eigenvector of \mathcal{T}_i .^{21,23)} For a fixed value of the Trotter time steps $\Delta\tau = \beta_0/N_0$, we then lower the temperature T by inserting additional time steps along the imaginary time direction between the system and environment parts of the transfer matrix \mathcal{T}_i . At the same time the dimension of the transfer matrix \mathcal{T}_i is kept tractable by applying the DMRG method and truncating the states with the smallest weight in the density matrix. The dimension of the Hilbert space can further be reduced by using symmetries such as the spin conservation symmetry and performing the calculations in the subspace of zero winding number.

In our calculations we usually keep $M = 80$ states for each of the system and environment blocks of the DMRG procedure, and estimate the truncation errors by comparing to the results with $M = 40$ and 60 states. For $M = 60$ states, the truncation error ε is always smaller than 10^{-3} . Another source of errors stems from the finite size of the Trotter time steps $\Delta\tau$. Basically one can extrapolate to $\Delta\tau \rightarrow 0$ by performing calculations for several different values of $\Delta\tau$. However, for doped systems, the TDMRG calculations need to be performed in the grand canonical ensemble, and the chemical potential μ is fixed for each DMRG iteration. Thus we need to extrapolate to constant particle density n afterwards, and for a large number of Trotter time steps N , the errors introduced by this extrapolation to constant particle density are in general larger than the errors caused by the finite size of the Trotter time steps. If not otherwise mentioned, we have therefore performed the calculations for fixed $\Delta\tau = 0.2t$ and neglected the errors caused by finite Trotter time steps. We have also used a re-biorthogonalization algorithm if we encounter numerical instabilities in the TDMRG procedure.²⁴⁾

Complementary to the TDMRG method, we have used the ground state DMRG method to investigate the correlation functions and ground-state energies. The main advantage of this method is that it allows very accurate calculations of these quantities for large $1D$ systems. We have investigated systems of up to 2×256 sites and kept up to $M = 1400$ states for the system and environment block each. The truncation errors encountered in our calculations are usually smaller than $\varepsilon < 10^{-8}$. All calculations have been performed on Alpha workstations at the ISSP.

§3. Results

3.1 Spin gap and magnetic properties

We start our investigations with the spin gap properties, and determine whether it remains finite upon doping for the different models. In the undoped case, both models can be mapped to the Haldane $S = 1$ chain for $J_H \gg J, J_d$. The effective coupling J_{eff} between the $S = 1$ spins is $J_{\text{eff}}^{\text{as}} = 3J/4$ for the asymmetric and $J_{\text{eff}}^{\text{sym}} = J$ for the symmetric model by second order perturbation theory, thus we expect a spin gap of $\Delta_s = 0.41050(1)J_{\text{eff}}$ in both cases.

By finite-size scaling we have numerically determined

n_h	Δ_s^{sym}	ξ^{sym}	$\Delta_s^{\text{sym+re}}$	$\xi^{\text{sym+re}}$	Δ_s^{as}	ξ^{as}	v_σ^{as}	χ_0
0	0.205(5) t	6.05(5)	0.205(5) t	6.05(5)	0.1504(5) t	6.05(5)	-	0
0.0625	0.148(5) t	6.1(2)	0.03(1) t	15.4(5)	0	7.9(2)	0.244	2.61
0.125	0.120(5) t	6.7(2)	0.02(1) t	20.5(5)	0	11.2(2)	0.201	3.17

Table I. Spin gap obtained by finite-size scaling analysis for the symmetric model (left), symmetric model with Coulomb repulsion $U = 10t$ (middle), and the asymmetric model (right) for $-J_H = 10t = 20J = 20J_d$. Also listed is the spin-spin correlation length ξ , and for the gapless asymmetric model the spin velocity v_σ and magnetic susceptibility χ_0 at $T = 0$. The definition of ξ is not simple for the cases with $\Delta_s = 0$, see text for details.

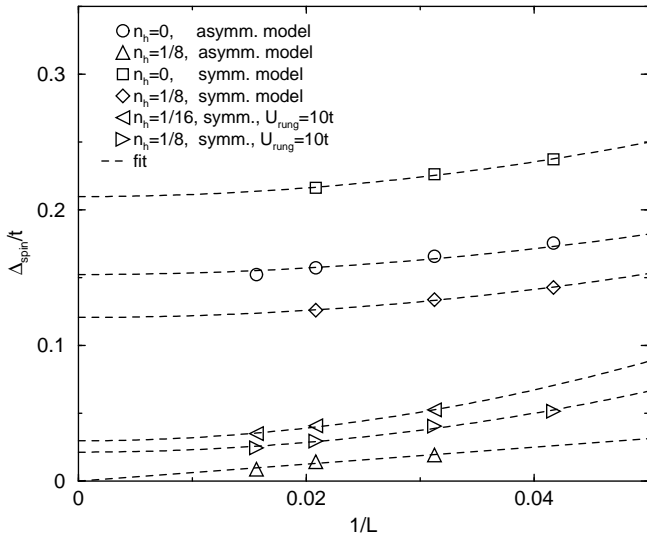


Fig. 1. Finite-size scaling of the spin gap Δ_s for the different models with $-J_H = 10t = 20J = 20J_d$, and $U = 10t$ for the model with Coulomb repulsion, and different hole densities of $n_h = 0$, $n_h = 1/8$, and $n_h = 1/16$.

the spin gap from $\Delta_s = \lim_{T \rightarrow 0} \Delta_s(L; N = Ln)$, where $\Delta_s(L; N = Ln) = \Delta_s(L; N) = E_0(L; N; S^z = 1) - E_0(L; N; S^z = 0)$ with $E_0(L; N; S^z)$ denoting the ground-state energy of the system with N particles on L sites and total spin component along the z -direction S^z . The result of the finite-size scaling analysis by DMRG calculations (see Fig. 1) is in excellent agreement with the above mapping, and we obtain $\Delta_s = 0.41(1)J_{\text{eff}}^{\text{as}} \approx 0.154(5)t$ in the asymmetric case and $\Delta_s = 0.41(1)J_{\text{eff}}^{\text{sym}} \approx 0.205(5)t$ for the symmetric model. In agreement with refs.^{15,16} we also find completely different behavior for both models upon doping, as is evident from Fig. 1 and we have listed the results in Table I. For the asymmetric model, the spin gap is completely destroyed already for hole densities of $n_h = 0.0625$ and $n_h = 0.125$, where n_h denotes the hole density in the conduction band. On the other hand, the gap is reduced, but remains finite for the symmetric model for the same hole densities $n_h = 0.0625$ and $n_h = 0.125$, where we set $n_h = 1 - n$ with n denoting the number of electrons per orbital for the symmetric models. The reduction of the spin gap is stronger in the symmetric case including a Coulomb repulsion $U = J_H$, but appears to remain finite. However, great care needs to be taken with the boundary conditions of the DMRG cal-

culations in order to avoid the degenerate $S = 1/2$ spin excitations at the end of the open chain, which would result in spin gaps exponentially small with the system-size L .¹⁹ By enumerating the sites of the open chain from $i = 1$ to L , we have used the boundary condition which enforces a $S = 1/2$ spin at site $i = 1$ and $S = 1$ at site $i = 2$, and similarly at the other end of the chain. If we do not enforce a $S = 1$ spin next to the $S = 1/2$ spins we find that holes are trapped at the boundary and the finite-size scaling becomes unreliable or impossible for smaller system sizes because of chain-end excitations.

From the finite-size scaling we can also determine the spin velocity and magnetic susceptibility χ at $T = 0$ of the gapless asymmetric model by noting that the smallest momentum in the finite open chain is $k_{\text{min}} = \pi/L$. The spin velocity v_σ can then be obtained from $\Delta_s(L) = v_\sigma k_{\text{min}}$, and the magnetic susceptibility is given by $\chi_0 = \frac{2K_\sigma}{\pi v_\sigma}$, where $K_\sigma = 1$ due to the SU(2) symmetry. We see from Table I that the magnetic susceptibility χ is rather large already for small values of hole doping.

Next we compare these findings for the magnetic susceptibility with the TDMRG results shown in Fig. 2 for the asymmetric model for $-J_H = 10t = 20J = 20J_d$, and we refer to Fig. 1 of ref. 17 for the symmetric model. For the symmetric model we have set $-J_H \rightarrow \infty$ to be able to keep enough states in the TDMRG algorithm (with $M = 100$ states). In the inset of Fig. 2 we show the convergence of the TDMRG method for several choices of the Trotter time steps $\Delta\tau$ and numbers of states kept for the example of $n_h = 0.125$. Keeping only $M = 45$ states is clearly not sufficient, and this curve deviates from the other curves already at rather high temperatures around $T \approx 0.3t$. The other curves with $M = 60$ and different values of $\Delta\tau$ show good convergence, but at the lowest temperatures an accurate estimate of the errors gets more difficult. In the figure for all hole densities we therefore only show χ down to temperatures where we estimate the truncation errors to be smaller than 1% and interpolation errors to constant particle density also smaller than 1%. The first observation is that both the symmetric and asymmetric model show a strong enhancement of χ at temperatures near the gap value of the undoped chain $T \propto J/2$. This strong enhancement of χ is caused by the creation of a small FM cloud around each mobile hole by the double exchange mechanism, as the holes can gain kinetic energy by FM alignment of the neighboring spins. At even lower temperatures, the magnetic susceptibility is suppressed

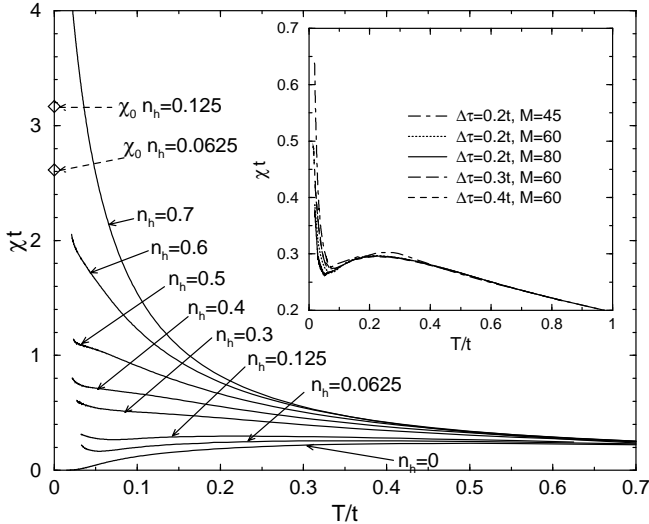


Fig. 2. Magnetic susceptibility χ of the asymmetric model for $-J_H = 10t = 20J = 20J_d$. The $T = 0$ values are obtained from the spin velocities obtained by a finite-size scaling analysis. In the inset we show the convergence of the TDMRG method for different sizes of the Trotter time steps $\Delta\tau$ and different numbers of states kept M for $n_h = 0.125$.

for the symmetric model due to the spin gap and we find $\chi \rightarrow 0$ for $T \rightarrow 0$. In contrast, χ is finite and rather large at $T = 0$ for the asymmetric model, indicating the formation of larger FM moments due to the double exchange mechanism (see ref. 13). However, the ground state is spin singlet for both models, as we have tested with the DMRG method by the calculation of $\sigma(i, j) = S_i^z S_j^z - 1/2(S_i^+ S_j^-)$ which vanishes for a rotationally invariant ground state and the result is zero within the numerical precision of the DMRG for this quantity for both models ($|\sigma(i, j)| < 10^{-6} \forall i, j$).

3.2 Spin correlation function

Complementary information about the magnetic properties can be gained from the spin-spin correlations $S_{\text{sp}}(i-j) = \langle S_i^z S_j^z \rangle$. For gapful systems we expect the spin-spin correlations to decay exponentially, whereas we expect power-law decay for gapless systems. By the DMRG method we have measured the spin-spin correlations for the different models on very large chains of up to 2×256 sites, and we show some of those calculations in Fig. 3. For the undoped system, the spin-spin correlations clearly exhibit the expected exponential decay, and by fitting to the asymptotic form $S_{\text{sp}}(l) \propto (-1)^l l^{-1/2} e^{-l/\xi}$ we obtain $\xi = 6.05(5)$ in agreement with the results for the Haldane $S = 1$ chain.¹⁹ For both gapful symmetric models we expect exponentially decaying spin-spin correlations also in the doped case. However, in Fig. 3 we observe an additional spiral-order in $S_i^z S_j^z$ on top of the exponential decay upon doping, and we fit to $S_{\text{sp}}(l) \propto \cos(2k_F l) e^{-l/\xi}$ in that case. The correlation lengths listed in Table I demonstrate that correlation lengths $\xi \approx 6.1(2)$ for $n_h = 0.0625$ and $\xi \approx 6.7(2)$ for $n_h = 0.0625$ are very close to the undoped case in the absence of the Coulomb repulsion, while the correlation

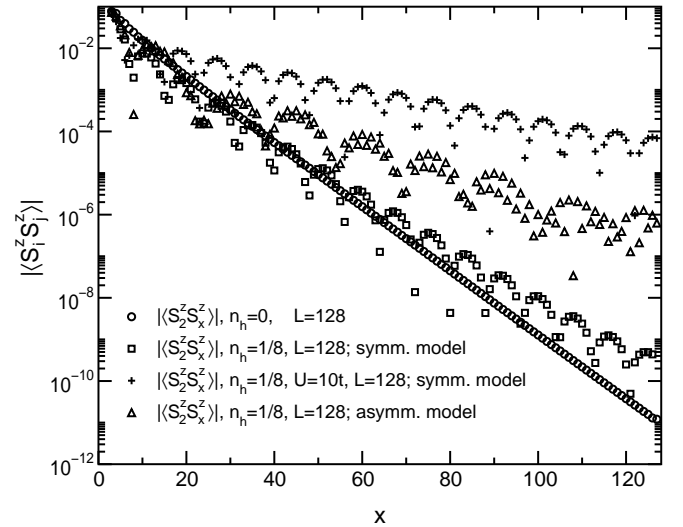


Fig. 3. Spin-spin correlation functions $S_i^z S_j^z$ at low hole doping $n_h = 0.125$ for the different models calculated by the DMRG method on 2×128 site systems and $-J_H = 10t = 20J = 20J_d$, and $U = -J_H$ for the symmetric model with Coulomb repulsion. For comparison we also show the undoped symmetric system.

length ξ increases by a factor of 2.56 to $\xi \approx 15.4(5)$ for $n_h = 0.0625$ and 3.41 to $\xi \approx 20.5(5)$ for $n_h = 0.125$ at $U = 10t$. Rather surprisingly, also for the gapless asymmetric model the spin-spin correlations seem to decay exponentially with correlation lengths $\xi = 7.9(2)$ for $n_h = 0.0625$ and $\xi = 11.2(2)$ for $n_h = 0.125$. This exponential decay of the spin-spin correlations at intermediate distances reflects the underlying spin-liquid background, and we expect a crossover to power-law decay at larger distances. However, since this length scale is given by the polaron-polaron distance, we can not discriminate between power-law and exponential decay due to the fact that even our largest systems contain few polarons only, and much larger systems would be required for that purpose.

This hierarchy of energy scales in the spin-sector of the asymmetric model should also be visible by two peaks in the specific heat c_V . First, we expect a large, broad peak around the gap-value Δ_s of the undoped $S = 1$ chain stemming from the spin-liquid background, and a second peak at low temperatures reflecting the lower gapless AF interactions among the polarons. This two-peak structure is evident in Fig. 4 of ref. 13 by a broad peak around $T \approx J$ reflecting the spin-liquid background and from the steep increase of c_V signaled at the lowest temperatures. We estimate an energy scale of $T < 0.02t$ for the magnetic interactions among the polarons.

3.3 String correlation function

The hidden $Z_2 \times Z_2$ symmetry of the Haldane $S = 1$ chain is revealed by the string correlation function $g(l) = \langle (S_{x_0}^z) \left(\prod_{k=x_0+1}^{x_0+l-1} e^{i\pi S_k^z} \right) (S_{x_0+l}^z) \rangle$, which quickly approaches the value $g(l) \approx -0.374$ for $l \gg 1$ in the undoped case.² As a natural extension for the doped

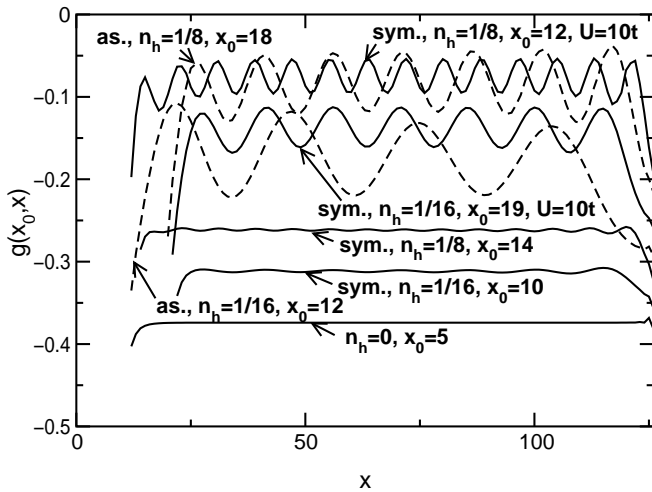


Fig. 4. String correlation function $g(x_0, x) = \langle (\sum_{i=1,2} S_{x_0,i}^z) (\prod_{k=x_0+1, j=1,2}^{x-1} e^{i\pi S_{k,j}^z}) (\sum_{l=1,2} S_{x,l}^z) \rangle$ at low hole doping for the different models with $-J_H = 10t = 20J = 20J_d$ and $U = -J_H$ for the symmetric model with Coulomb repulsion obtained by DMRG calculations on systems with 2×128 sites.

models we consider

$$g(x) = \left\langle \left(\sum_{i=1,2} S_{x_0,i}^z \right) \left(\prod_{k=x_0+1, j=1,2}^{x-1} e^{i\pi S_{k,j}^z} \right) \left(\sum_{l=1,2} S_{x,l}^z \right) \right\rangle, \quad (3.1)$$

and the results are shown in Fig. 4. In the undoped case we quickly recover the original result of $g(l) \approx -0.374$ for $l \gg 1$. The value of $g(l)$ is only slightly reduced to $g(l) \approx -0.31(2)$ for $n_h = 0.0625$, and $g(l) \approx -0.26(2)$ for $n_h = 0.125$ for the symmetric model without Coulomb repulsion in agreement with the weak-coupling result of ref. 15. Combined with the very small deviation in the spin correlation length ξ from the undoped case, we conclude that the spin structure of the symmetric model is very similar to that of the undoped $S = 1$ Haldane chain. The suppression of the string correlation function $g(l)$ is much stronger if we include the Coulomb repulsion or for the asymmetric model and we obtain $g(l) < 0.1$ for both of these models for $n_h = 0.125$. In addition, the latter two models also exhibit large oscillations in the amplitude of $g(x)$, caused by the Friedel oscillations in the charge density due to the open boundary conditions. By comparison $g(l)$ is constant within 1.2% for the symmetric model without Coulomb repulsion apart from boundary effects. In fact, for the asymmetric model we again expect a crossover to power-law decay of $g(l)$ after sufficiently many oscillations.

3.4 Friedel oscillations and correlation exponent

Friedel oscillations are induced in the charge density due to the open boundary conditions. For gapful Luther-Emery and gapless Tomonaga-Luttinger liquids, we can then obtain from these oscillations the correlation exponent K_ρ which determines the dominant correlation functions in the thermodynamic limit.

We first consider the Fourier-transform of the charge density shown in the inset of Fig. 5. For both of the

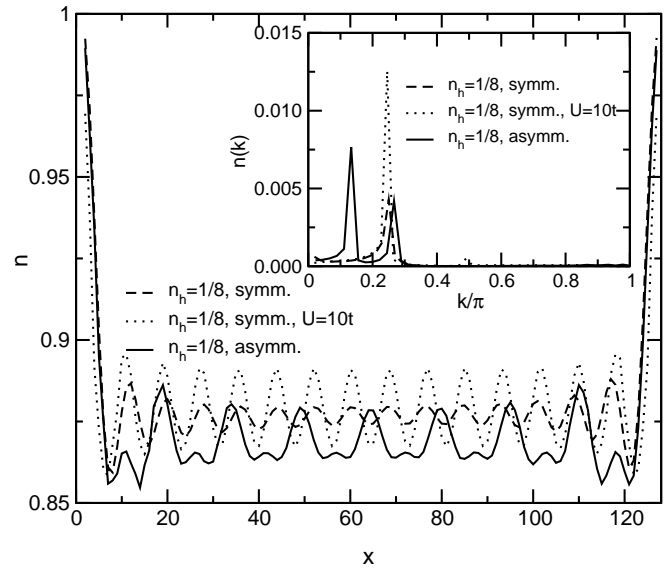


Fig. 5. Friedel oscillations in the charge density distribution due to the open boundary conditions for the different models with $-J_H = 10t = 20J = 20J_d$ at low hole doping $n_h = 0.125$. In the inset we show the corresponding Fourier transform.

symmetric models we find only one peak at $k = 2n\pi$. Since the lower band is fully occupied for low hole densities, there are $N_h^{\text{up}} = 2(1-n)L$ holes in the upper band and its particle density is $n^{\text{up}} = 2n - 1$. For large Fermi volume, the Fermi vector is thus given by $2k_F = \pi + (2n - 1)\pi = 2n\pi$ and the above peak is compatible with $2k_F$ oscillations. For the asymmetric model we find only one peak at $k = n_h\pi$ at the smallest hole density $n_h = 0.0625$, but two peaks at $k = n_h\pi$ and $k = 2n_h\pi$ for $n_h = 0.125$ as is evident in Fig. 5. Since we denote the hole density in the conduction band with n_h in this case, we obtain a Fermi vector of $2k_F = \pi + (1 - n_h)\pi \equiv n_h\pi$ for a large Fermi volume and the above peaks are compatible with $2k_F$ and $4k_F$ oscillations.

After having identified the $2k_F$ and $4k_F$ fluctuations, we determine the correlation exponent by fitting to the Friedel oscillations of an impurity potential. In the gapful case they are given by $\delta_n(x) \propto C_1 \cos(2k_F x) x^{-K_\rho} + C_2 \cos(4k_F x) x^{-2K_\rho}$ and $\delta_n(x) \propto C_1 \cos(2k_F x) x^{-(1+K_\rho)/2} + C_2 \cos(4k_F x) x^{-2K_\rho}$ in the gapless case.²⁵⁾ For both gapful and gapless universality classes, a value of $K_\rho > 1$ leads to dominant pairing correlations in the thermodynamic limit, while the CDW correlations decay slowest for $K_\rho < 1$. From Fig. 5 it is evident that the amplitudes of the symmetric model without Coulomb repulsion decay much faster than for the other models where they are almost constant. For the fit we have to discard the states next to the boundary because of trapped states. For the symmetric model without Coulomb repulsion we find by fitting to the gapful Luther-Emery liquid $K_\rho \approx 1.5 \pm 0.05$ for $n_h = 0.125$, showing dominant pairing correlations, and $K_\rho \approx 0.41 \pm 0.08$ upon the inclusion of a Coulomb repulsion of $U = 10t$, giving dominant CDW correlations. For the asymmetric model we fit to the gapless Tomonaga-Luttinger liquid and find

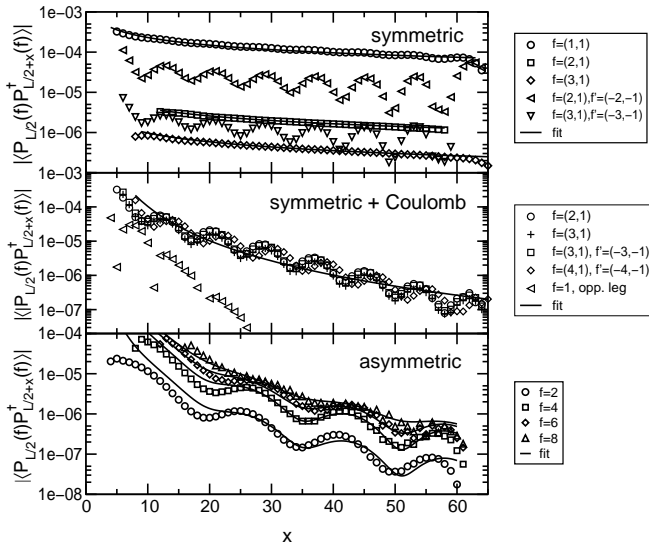


Fig. 6. Singlet pairing correlations $P_i(f)P_{i+x}^\dagger(f')$ with $P_i^\dagger(f) = \frac{1}{\sqrt{2}}(c_{i,\uparrow}^\dagger c_{i+f,\downarrow}^\dagger - c_{i,\downarrow}^\dagger c_{i+f,\uparrow}^\dagger)$ for (a) symmetric model, (b) symmetric model with Coulomb repulsion $U = 10t$, and (c) asymmetric model at $n_h = 1/8$ and $-J_H = 10t = 20J = 20J_d$.

$K_\rho \approx 0.51 \pm 0.05$, also at $n_h = 0.125$. Pair formation can be explained by the gain of the large Hund's rule coupling for holes pairs formed on the rungs of the symmetric model. This energy gain is not possible for both of the other models, and in contrast the holes may gain kinetic energy by the double exchange mechanism in these cases. In the low hole doping region we can determine hole pairing from the pair binding energy obtained from $\Delta_{\text{pair}} = 2E_1 - E_0 - E_2$, with E_n denoting the ground-state energy with n holes. For the symmetric model without Coulomb repulsion we confirm hole pairing by a large binding energy of $\Delta_{\text{pair}} \approx 2.29t$. Including the Coulomb repulsion, the holes repel each other and we obtain $\Delta_{\text{pair}} \approx -0.07t$, while the asymmetric model shows a very small positive binding energy of $\Delta_{\text{pair}} \approx 0.016t$ near half-filling. Pair binding has also been found in ref.¹²⁾ in a similar model.

3.5 Pairing correlations

Independently of the Friedel oscillations in the charge density, we can also determine the correlation exponent from the pairing correlations defined as $P_i(\vec{f}')P_{i+x}^\dagger(\vec{f})$, where $P_i^\dagger(\vec{f}) = \frac{1}{\sqrt{2}}(c_{i,\uparrow}^\dagger c_{i+\vec{f},\downarrow}^\dagger \mp c_{i,\downarrow}^\dagger c_{i+\vec{f},\uparrow}^\dagger)$ either denotes the singlet ($-$) or the triplet pair ($+$) creation operator. The pairing correlations also give further information on the form-factor \vec{f} . For gapful models belonging to the universality class of Luther-Emery liquids, the pairing correlations decay as $P_i(f)P_{i+x}^\dagger(f) \propto x^{-1/K_\rho}$,²⁶⁾ whereas for gapless Tomonaga-Luttinger liquids the asymptotic form is given by $P_i(f)P_{i+x}^\dagger(f) \propto A_0 \ln(x)^{-1.5} x^{-1-1/K_\rho} + A_2 \cos(2k_F x) x^{-K_\rho-1/K_\rho}$.²⁷⁾

In Fig. 6 we show the singlet pairing correlations obtained from our DMRG calculations on systems with 2×128 sites. From the numerous possibilities of the form-factor \vec{f} for the symmetric model, we restrict the discussion to those with the largest amplitudes in the fol-

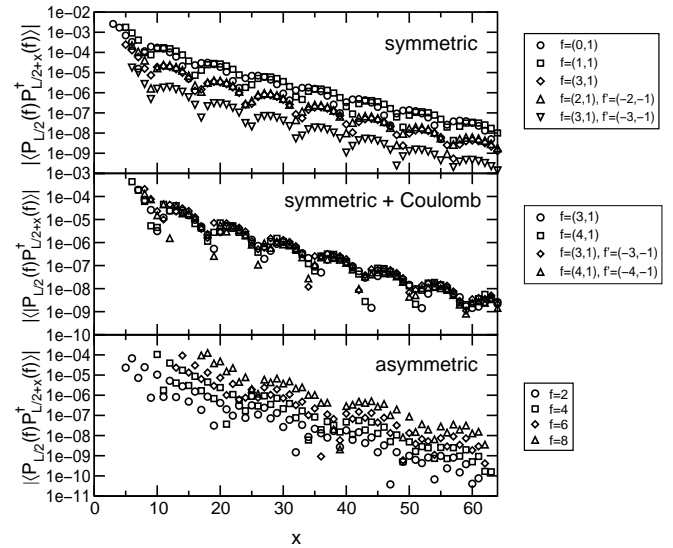


Fig. 7. Triplet pairing correlations $P_i(f)P_{i+x}^\dagger(f')$ with $P_i^\dagger(f) = \frac{1}{\sqrt{2}}(c_{i,\uparrow}^\dagger c_{i+f,\downarrow}^\dagger + c_{i,\downarrow}^\dagger c_{i+f,\uparrow}^\dagger)$ for (a) symmetric model, (b) symmetric model with Coulomb repulsion $U = 10t$, and (c) asymmetric model at $n_h = 1/8$ and $-J_H = 10t = 20J = 20J_d$.

lowing. In excellent agreement with the previous results for K_ρ we find $K_\rho \approx 1.55 \pm 0.05$ for the symmetric model without Coulomb repulsion at $n_h = 0.125$. The form factor of the pairs with largest amplitudes $\vec{f} = (1, 1)$, $(2, 1)$ and $(3, 1)$ are consistent with a d_{x-y} symmetry analogue for a ladder. Surprisingly there are also almost no $2k_F$ oscillations in the pairing-correlations for the largest amplitudes, despite the Friedel oscillations in the charge density.

Upon the inclusion of the Coulomb repulsion, the pairing correlations decay much faster and in agreement with the previous result from the Friedel oscillations we obtain $K_\rho \approx 0.42$. Finally by simultaneously fitting to $f = 2, 4, 6$, and 8 for a Tomonaga-Luttinger liquid, we obtain $K_\rho \approx 0.51 \pm 0.05$ for the asymmetric model at $n_h = 0.125$. The form factor of the pairing correlations with the largest amplitudes is $f = 8$ and $f = 6$ in this case. Rather extended pair formation is also evident from a corresponding, weak substructure at a distance of $d = 8$ in the hole pockets of the charge density distribution in Fig. 5.

The triplet pairing correlations decay exponentially for both universality classes. The correlations for the form factors f with the largest amplitudes are shown in Fig. 7 for systems with 2×128 sites and $P_i^\dagger(\vec{f}) = \frac{1}{\sqrt{2}}(c_{i,\uparrow}^\dagger c_{i+\vec{f},\downarrow}^\dagger + c_{i,\downarrow}^\dagger c_{i+\vec{f},\uparrow}^\dagger)$. The correlation functions for the other triplet states are similar. At very short distances $d < 5$, triplet pairing correlations for rung pairs with $\vec{f} = (0, 1)$ and $\vec{f} = (1, 1)$ have the largest amplitudes for the symmetric model without Coulomb repulsions, but since they decay exponentially fast, the amplitudes for singlet pair correlations become larger for distances $d > 5$. Including the Coulomb repulsion $U = 10t$, the singlet correlations always have larger amplitudes. For the asymmetric model, the triplet correlations have the largest amplitudes for short distances $d \lesssim 5$ with

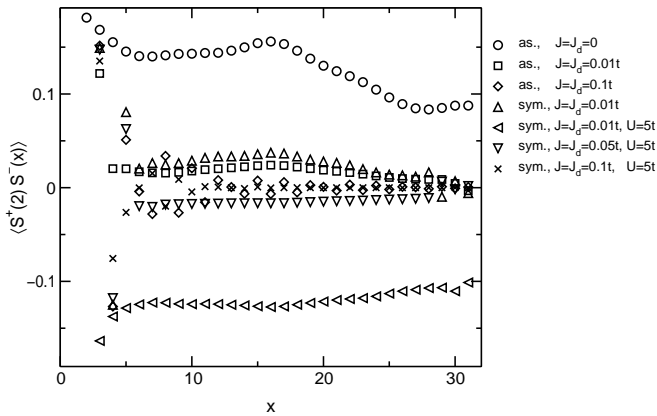


Fig. 8. Spin-spin correlations in the $x-y$ plane for the asymmetric model and symmetric model for $S_{\text{tot}}^z = 0$ with $J_H = -10t$, $L = 32$, $n_h = 0.125$ and various values of J, J_d , calculated by the DMRG method.

a form-factor of $f = 4$, but again, the singlet correlations become dominant at larger distances $d > 5$ due the exponential decay of the triplet correlations.

3.6 Ferromagnetism and triplet pairing

Ferromagnetism induced by the double-exchange mechanism is to be expected for the asymmetric model and the symmetric model with Coulomb repulsion at $J = J_d = 0$, and might extend to small, but finite values of J, J_d . Rather large FM regions have been identified in the phase diagrams of refs. 12, 28 for related models.

In a first approach we determine the FM region by comparing ground-state energies in different total S_{tot}^z subspaces calculated by the DMRG method. In the FM phase, all the spins are fully aligned and the ground state is compatible with $S_{\text{tot}}^z = (2L - N_h)/2$, while for singlet ground state with N_h even, $S_{\text{tot}}^z = 0$ is lowest in energy, where N_h denotes the number of holes in the system of length L . Because of the number of subspaces with different S_{tot}^z becomes very large for large system sizes, we can do such calculations only for rather small systems, and we have used $L = 32$ for our calculations. For the asymmetric and the symmetric model with $U = 5t$, $S_{\text{tot}}^z = 0$ is lowest in energy for $J = J_d \gtrsim 0.1t$, and $S_{\text{tot}}^z = (2L - N_h)/2$ is lowest for $J = J_d = 0$. For intermediate values $0 < J, J_d < 0.1t$ some $0 < S_{\text{tot}}^z < (2L - N_h)/2$ is lowest in energy. While these results clearly demonstrate a singlet groundstate for $J = J_d \gtrsim 0.1t$ and a FM groundstate for $J = J_d = 0$, the results are not conclusive for the intermediate region, due to the special boundary conditions required to suppress the chain-end excitations.

An alternative approach to determine the FM region is possible by the spin-spin correlations. Working in the $S_{\text{tot}}^z = 0$ subspace, the spins are ferromagnetically aligned in the $x-y$ plane in the FM phase. In Fig. 8 we show the $S^+(2)S^-(x)$ correlations for the asymmetric model and the symmetric model with $U = 5t$ calculated by the DMRG method for a system size of $L = 32$ sites. In the asymmetric model, all the spins are fully ferromagnetically aligned for $J = J_d = 0$. Ferromagnetic

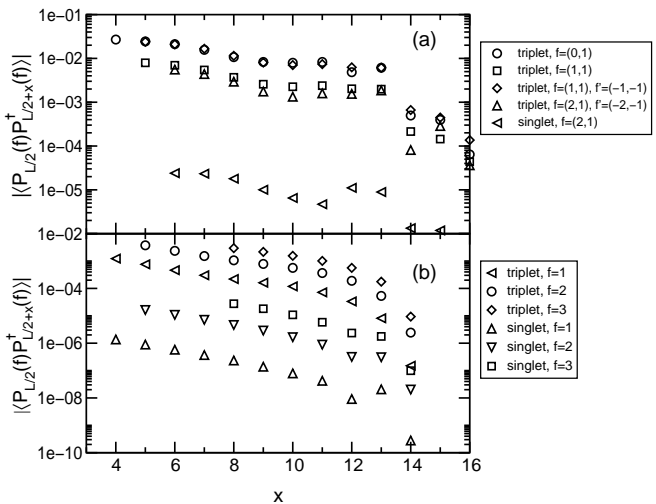


Fig. 9. Pairing correlation functions $P_i(f)P_{i+x}^\dagger(f')$ with $P_i^\dagger(f) = \frac{1}{\sqrt{2}}(c_{i,\uparrow}^\dagger c_{i+f,\downarrow}^\dagger \mp c_{i,\downarrow}^\dagger c_{i+f,\uparrow}^\dagger)$ in the FM phase for (a) symmetric model, and (b) asymmetric model at $n_h = 1/8, J_H = -10t$ and $J = J_d = 0.01t$.

alignment of the spins is still evident for $J = J_d = 0.01t$, however at the end of the chain, the last spin is antiferromagnetically aligned. For $J = J_d = 0.1t$, we find AF alignment compatible with the singlet groundstate. The same situation is encountered also for the symmetric model with $U = 5t$, where we find fully polarized spins for $J = J_d = 0.01t$, a few spins at the boundary with AF alignment for $J = J_d = 0.05t$, and AF alignment for $J = J_d = 0.1t$, where the period of the AF alignment corresponds to $2k_F$ oscillations. Without Coulomb repulsion, the FM phase seems to be slightly reduced, since the strong pair binding on the rungs reduces the double exchange mechanism. Already for $J = J_d = 0.01t$ a few spins are antiferromagnetically aligned in this case, but the bulk is still ferromagnetically aligned. The AF alignment of the spins at the boundaries is expected to be a finite-size effect only and can be explained by the decreased mobility of the holes near the boundaries, which in turn reduces the double-exchange mechanism and favors AF order. At $J_H = 10t$ we therefore expect a narrow FM region for all models for $0 \leq J = J_d \lesssim 0.1t$.

The possibility of triplet superconductivity in the FM phase is a question of great interest and we have investigated this problem by the pairing correlation shown in Fig. 9. As is evident from the figure, the triplet pairing correlations for the symmetric model with $J_H = -10t$, and $J = J_d = 0.01t$ at $n_h = 0.125$ for a triplet pair $P_i^\dagger(\vec{f}) = \frac{1}{\sqrt{2}}(c_{i,\uparrow}^\dagger c_{i+\vec{f},\downarrow}^\dagger + c_{i,\downarrow}^\dagger c_{i+\vec{f},\uparrow}^\dagger)$ formed on a rung are roughly three orders of magnitude larger than the largest singlet pairing correlations, and at least for this system size, do not seem to decay faster than the singlet pairing correlations. Also for the asymmetric with the same parameters, the triplet pairing correlations are roughly three orders of magnitude larger than the singlet pairing correlations, and do not seem to decay faster than the singlet pairing correlations. From the system sizes in our study it is not possible to distinguish between exponential or power-law decay, but at least for the 2×32

systems, dominant triplet pairing seems possible. Larger system sizes are needed in order to determine which correlation function decays slowest in the thermodynamic limit of infinite system size.

§4. Conclusions

In our study we have investigated three realistic models of AF $S = 1$ Heisenberg chains doped with mobile $S = 1/2$ fermions in the strong coupling regime: a model with a level difference between the two orbitals forming the $S = 1$ spins, a model without level difference, and a model without level difference including a strong Coulomb repulsion between the electrons in the two orbitals on the same site. Our investigation by numerical methods shows very different physical properties of these models.

For the asymmetric model with a level difference between the two orbitals, the spin gap is destroyed immediately upon doping, while it remains finite for both symmetric models with equal particle density in both orbitals. This collapse of the spin gap in the asymmetric model is caused by AF interactions among the polarons. The polarons are created by the double-exchange mechanism in order to gain kinetic energy, and if the AF couplings between the neighboring sites are $J, J_d = 0$, the ground state is FM. We also find evidence for a FM ground state for very small values of $J, J_d \lesssim 0.05t$ for all models. The absence of interactions among the polarons in the symmetric model lead to a finite spin gap in that case.

However, even for the asymmetric model the holes are only a weak perturbation of the underlying spin liquid. A hierarchy of energy scales is thus given in the spin sector of the asymmetric model by the lowest-lying, gapless AF interactions among the polarons and second, larger energy scale of the order of the spin gap of the undoped system by the underlying spin liquid which remains intact. As a consequence of the spin liquid background, the spin-spin correlations decay exponentially fast for all models for the system sizes in our study (up to 2×256 sites). However, we expect a crossover to power-law decay for the asymmetric at large distances. Also the string correlation function, which quickly approaches a nonzero value of the long-ranged order in the undoped system, remains finite for all models. Again, we expect a crossover to power-law decay for the asymmetric model at large distances.

Since hole pairing on the rungs is only possible for the symmetric model without strong Coulomb repulsion, we find completely different dominant correlations functions in thermodynamic limit of infinite system size. The symmetric model shows dominant pairing correlations and $K_\rho > 1$ without Coulomb repulsion, in contrast to dominant CDW correlations with $K_\rho < 1$ for the symmetric model with Coulomb repulsion and for the asymmetric model. In the FM region for small values of the AF interactions $J, J_d \lesssim 0.05t$, the triplet pairing correlations are strongly enhanced.

Acknowledgements

We wish to thank H. Asakawa and H. Tsunetsugu for valuable discussions. The numerical calculations have been performed on workstations at the ISSP. This work is supported by the ‘‘Research for the Future Program’’ (JSPS-RFTF 97P01103) from the Japan Society for the Promotion of Science (JSPS).

-
- 1) F.D. Haldane: Phys. Lett. **93A** (1983) 464; Phys. Rev. Lett. **50** (1983) 1153.
 - 2) M. den Nijs and K. Rommelse: Phys. Rev. B **40** (1989) 4709; S.M. Girvin and D.P. Arovas: Phys. Scr. **27** (1989) 156; H. Tasaki: Phys. Rev. Lett. **66** (1991) 798.
 - 3) C. Zener: Phys. Rev. **82** (1951) 403; P. W. Anderson and H. Hasegawa: Phys. Rev. **100** (1955) 675; P.-G. de Gennes: Phys. Rev. **118** (1960) 141.
 - 4) J.F. DiTusa *et al.*: Phys. Rev. Lett. **73** 1857 (1994).
 - 5) D.J. Buttrey, J.D. Sullivan, and A.B. Rheingold: J. Solid State Chem. **88** (1990) 291; J. Amador *et al.*: Phys. Rev. B **42** (1990) 7918; R. Sáez-Puche *et al.*: J. Solid State Chem. **93** (1991) 461; J. Darriet and L.P. Regnault: Solid State Commun. **86** (1993) 409; B. Battlogg, S.-W. Cheong, and L.W. Rupp, Jr.: Physica B **194-196** (1994) 173.
 - 6) K. Kojima *et al.*: Phys. Rev. Lett. **74** (1995) 3471.
 - 7) E.S. Sørensen and I. Affleck: Phys. Rev. B **51** (1995) 16115.
 - 8) M. Kaburagi, I. Harada, and T. Tonegawa: J. Phys. Soc. Jpn. **62** (1993) 1848; M. Kaburagi, and T. Tonegawa: J. Phys. Soc. Jpn. **63** (1993) 420.
 - 9) T. Kennedy: J. Phys. Condens. Matter **2** (1990) 5737.
 - 10) K. Penc, and H. Shiba: Phys. Rev. B **52** (1995) R715.
 - 11) E. Dagotto, J. Riera, A. Sandvik, and A. Moreo: Phys. Rev. Lett. **76** (1996) 1731; C.D. Batista, A.A. Aligia, and J. Eroles: Phys. Rev. Lett. **81** (1998) 4027; E. Dagotto, and J. Riera: Phys. Rev. Lett. **81** (1998) 4082.
 - 12) J. Riera, K. Hallberg, and E. Dagotto: Phys. Rev. Lett. **79**, (1997) 713.
 - 13) B. Ammon and M. Imada: Phys. Rev. Lett. (to be published).
 - 14) H. Frahm, M. P. Pfannmüller, and A. Tsvelik: Phys. Rev. Lett. **81** (1998) 2116; H. Frahm and S. Sobiella: Phys. Rev. Lett. **83** (1999) 5579; H. Frahm and N. A. Slavanov: preprint cond-mat/9912319.
 - 15) S. Fujimoto and N. Kawakami: Phys. Rev. B **52** (1995) 6189.
 - 16) N. Nagaosa and M. Oshikawa: J. Phys. Soc. Jpn **65** (1996) 2241.
 - 17) B. Ammon and M. Imada: J. Phys. Soc. Jpn **69** (to be published).
 - 18) R.J. Bursill, T. Xiang, and G.A. Gehring: J. Phys. Cond. Matt. **8** (1996) L583; X. Wang and T. Xiang: Phys. Rev. B **56** (1997) 3177; N. Shibata: J. Phys. Soc. Jpn. **66** (1997) 2221.
 - 19) S.R. White: Phys. Rev. Lett. **69** (1992) 2863.
 - 20) S.R. White: Phys. Rev. B **48** (1993) 10345.
 - 21) H. Betsuyaku: Prog. Theor. Phys. **73** (1985) 319; T. Yokota and H. Betsuyaku: Prog. Theor. Phys. **75** (1986) 46.
 - 22) H.F. Trotter: Proc. Am. Math. Soc. **10** (1959) 545; M. Suzuki: Prog. Theor. Phys. **56** (1976) 1454.
 - 23) M. Troyer, H. Tsunetsugu, and D. Würtz: Phys. Rev. B **50** (1994) 13515.
 - 24) B. Ammon, M. Troyer, T.M. Rice, and N. Shibata: Phys. Rev. Lett. **82** (1999) 3855.
 - 25) M. Fabrizio and A.O. Gogolin: Phys. Rev. B **51** (1995) 17827; R. Egger and H. Grabert: Phys. Rev. Lett. **75** (1995) 3505; R. Egger and H. Schoeller: Czech. J. Phys. **46** (1996) Suppl. S4, 1909.
 - 26) A. Luther and V.J. Emery: Phys. Rev. Lett. **33** (1974) 589.
 - 27) J. Sólyom, Adv. Phys.: **28** (1979) 201; V.J. Emery: *Highly Conducting One-Dimensional Solids*, (Plenum, New York 1979), edited by J.T. Devreese *et al.*.
 - 28) K. Kubo *et al.*: preprint cond-mat/9811286.